

Modes of speciation in heterogeneous space

Martin Rost¹ and Michael Lässig²

¹*Abteilung Theoretische Biologie, Universität Bonn, Kirschallee 1, 53115 Bonn*

²*Institut für Theoretische Physik, Universität zu Köln, Zùlpicher Straße 77, 50937 Köln*

November 1, 2018

Abstract

Modes of speciation have been the subject of a century's debate. Traditionally, most speciations are believed to be caused by spatial separation of populations (*allopatry*). Recent observations [1, 2, 3, 4] and models [5, 6, 7, 8, 9, 10, 11, 12, 13, 14, 15], show that speciation can also take place in *sympatry*. We discuss a comprehensive model of coupled differentiation in phenotype, mating, and space, showing that spatial segregation can be an induced process following a sympatric differentiation. This is found to be a generic mechanism of adaptation to heterogeneous environments, for which we propose the term *diapatric* speciation [16]. It explains the ubiquitous spatial patching of newly formed species, despite their sympatric origin [2, 3, 4].

Allopatric speciation occurs in populations extending over a sufficient range in space and time. If subpopulations become spatially isolated, they can diverge in phenotype by adaptation to different environments as well as by genetic drift. A similar divergence is possible while the subpopulations maintain a limited spatial contact [7, 17, 18, 19, 20], which is commonly referred to as *parapatric* speciation. Pre- or post-mating incompatibilities can develop subsequently, leading to reproductive isolation. Neither the primary phenotypic separation nor the secondary reproductive isolation require disruptive selection. Hence, allopatric or classical parapatric speciation may well take too much space and time to account for radiation events and rapid species divergence [21, 22].

In recent years, phylogeographic observations have produced convincing evidence for speciation in sympatry. Reproductive isolation has occurred in cichlid populations in African lakes over a few thousand generations [1, 2, 3]. A salmon population is reported to have separated within only 14 generations [23]. Sympatric speciation thus appears to occur rapidly even in small contiguous environments without spatial barriers. In theoretical models, it is always driven by *disruptive selection*. A phenotypic split can be favored, for example, if individuals of similar phenotype compete more strongly than distant ones [8, 11]. In a sexually reproducing population, however, such splits can only happen if the subpopulations become reproductively isolated so that the birth of hybrids is suppressed [5, 8, 9, 15]. Of course, the sympatric scenario cannot explain the spatial population structure observed in the phylogeographic studies. Spatial patching of subpopulations appears to be ubiquitous. For example, the sister species of cichlids tend to organize themselves into neighboring regions [3, 4, 24]. Another well-documented case are phytophagous insects, which are found to evolve mating assortativity together with specificity to different host plants [25].

These observations call for a more comprehensive model that captures the divergence in phenotypic traits, mating, and space as a cooperative dynamical process. Only recently

IBM simulations in an extended model space with environmental fitness gradient have been presented [26] extending previous studies with complete spatial mixing [13, 14].

The model discussed here addresses parapatric speciation, i.e., generic intermediate cases between sympatry and allopatry. It affords a detailed analysis of the dynamics, allowing us to identify different primary speciation mechanisms and their conditions of occurrence. (A concise discussion of classification issues and of the appropriate terminology can be found in Ref. [21].) It turns out that the basic evolutionary forces driving speciation can be captured by a deterministic “reaction-diffusion” approach. We also discuss the role of stochastic effects as they appear in individual-based models. In this way, we recover the well-known mechanisms of allopatric and sympatric speciation. However, there are many environments with inhomogeneities on smaller scales in space and time (such as in the examples quoted above), where spatial variations prevent sympatry and diffusive migration prevents allopatry. Adaptive evolution then operates by a new mechanism, for which we propose the term *diapatric speciation*. The population reaches a final state of efficient spatial patchiness and phenotypic differentiation without hybrids, which is triggered and sustained by assortative mating. This is in contrast to the traditional view of parapatric speciation, where assortative mating takes a merely secondary role in reinforcing an existing boundary between emerging species [17, 18, 20, 21].

Model

We consider a population via its *density* in “internal” and “external” space, $N \equiv N(\mathbf{x}; \mathbf{r}; t)$. Internal coordinates $\mathbf{x} = (x_1, \dots, x_n)$ denote phenotypic quantities, e.g., body size, beak length, colour. Internal coordinates can be inherited. This representation is purely phenotypic. A comparison with explicitly genetic models is given below.

External coordinates $\mathbf{r} = (r_1, \dots, r_d)$ lie in the simplest case in d -dimensional Euclidean space. More complicated geometries, e.g., network structures of habitat patches in fragmented landscapes, are also possible. In this work, we focus on habitats with a gradient in quality for different phenotypes, which induce a spatial dependence of the optimal phenotype $\mathbf{x}_{\text{opt}}(\mathbf{r})$ and a population density $N(\mathbf{x}, \mathbf{r}; t)$ with a *joint* dependence on internal coordinates \mathbf{x} and external coordinates \mathbf{r} .

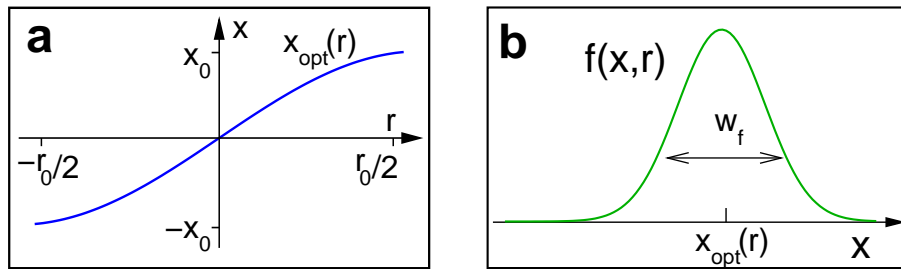


Figure 1: The fitness landscape of a heterogeneous model environment involves a fitness function $f(x, r)$ that depends on a trait variable x and a spatial coordinate r . (a) The left region ($r < 0$) favors smaller values of x , the right region ($r > 0$) larger ones. The optimal trait $x_{\text{opt}}(r)$ varies between the values $\pm x_0$ over a spatial interval given by the total size r_0 . (b) At a given point r , the fitness is maximal at $x_{\text{opt}}(r)$ and decays rapidly over a characteristic scale w_f , called the niche width.

In the simplest version of the model we consider one phenotypic coordinate and a one-dimensional external space of size r_0 , so $N \equiv N(x, r; t)$ with $-r_0/2 \leq r \leq r_0/2$. The

phenotype x is directly related to an ecological fitness or carrying capacity, e.g., with the explicit choice

$$f(x, r) = f(x - x_{\text{opt}}(r)) = \exp\left(-\frac{(x - x_{\text{opt}}(r))^2}{w_f^2}\right) \quad (1)$$

which is taken to be constant in time. It decreases with the distance of x from $x_{\text{opt}} = x_0 \sin(\pi r/r_0)$, on a scale w_f in phenotype space. x_0 is a measure for habitat heterogeneity and r_0 is the spatial scale of variation. For an illustration see Figure 1.

The population $N(x, r; t)$ is subject to the dynamics

$$\partial_t N(x, r; t) = \lambda \partial_r^2 N(x, r; t) + R(x, r; t) + (f(x, r) - K(x, r; t)) N(x, r; t) \quad (2)$$

which has the form of a reaction-diffusion equation.

The simplest type of motion in the population is diffusion, in Eq. (2) appearing as the term $\lambda \partial_r^2 N$, to which we restrict ourselves in this work. The prefactor defines a length scale in space, $r_\lambda = \sqrt{\lambda}$, which has to be compared with the habitat size r_0 .

The special case of eq. (2) with $R = 0$ describes the dynamics of an asexual or clonal population. It similar to the familiar Lotka-Volterra form. The resource supply $f(x, r)$ and the competition load

$$K(x, r; t) = \int dy \beta(x, y) N(y, r; t), \quad (3)$$

which sums up the influence of individuals of trait y on those with trait x , combine to the frequency-dependent *fitness* $f - K$. The competition kernel

$$\beta(x, y) = \beta(|x - y|) = \exp\left(-\frac{|x - y|}{w_\beta}\right) \quad (4)$$

is maximal for $x=y$ and decays on a scale w_β in internal space.

Extending this approach to sexually reproducing populations requires a more detailed model for birth processes, whose rate itself becomes dependent on the maternal and paternal population densities. It is convenient to introduce the *birth excess* per phenotype, space, and time

$$R(x, r; t) = \int dy dz C(x|y, z) m(y, z; t) N(z, r; t) - N(x, r; t). \quad (5)$$

by summing over the density of possible mothers $N(z, r; t)$ multiplied by the probability density $m(y, z)$ for a z -female to mate with a y -male and the inheritance probability density $C(x|y, z)$ that this couple will have offspring of phenotype x . The subtracted term $N(r, t)$ describes the total birth rate in the clonal limit. With the definitions of C and m given below, it is easy to check that $\int dx R(x, r) = 0$. Hence, the excess birth rate describes the net *reshuffling* of population density through sexual reproduction, and $f - K$ remains a useful measure of the frequency- and space-dependent fitness. The genetic function C is approximated by a Gaussian, $C(x|y, z) = \exp(-(x - \bar{x})^2 / (2w_C(\bar{x})^2)) / \sqrt{2\pi w_C(\bar{x})^2}$, with $\bar{x} = (y+z)/2$, so offspring is distributed near the mean of the parents' phenotype. Moreover the standard deviation $w_C(\bar{x})$ changes little over the relevant range of phenotypes. This form can be justified from the hypergeometric model [27, 28, 29, 30], where the quantitative trait x is encoded by L independent two-allele loci with equal allele frequencies. However, provided the number of independent loci is sufficiently large, it remains valid more generally, even if (i) the number of loci changes or (ii) the symmetry between the loci is lost [31] because allele frequencies change or linkage disequilibria develop during

the speciation process. Typically this would result in a decrease of w_C , but as long as $w_C < w_f$ and $w_C < w_\beta$, variations in w_C do not influence the results significantly. See also the discussion at the end of this Section where we show that this form of $C(x|y, z)$ emerges from a genetically explicit model quite generically.

Mating preference is crucial for the development of any structure in the population. Without it, the mating probability is just proportional to the available males. In this case the entire population is mixing and forms a single cluster in phenotype, see Figure 3(a). This changes with an affinity of females towards certain types of males,

$$m(y, z; t) = \frac{\mu(y, z)N(y, r; t)}{\int_w \mu(w, z)N(w, r; t)}. \quad (6)$$

Here we restrict ourselves to assortative mate choice by the ecological trait within a range of width w_μ

$$\mu(y, z) = \mu(|x - y|) = \exp\left(-\frac{|x - y|^2}{w_\mu^2}\right). \quad (7)$$

With strong enough mating assortativity reproductively isolated subpopulations can co-exist, as shown in Figure 3(b).

The population dynamics (2) always leads to a stationary density $\bar{N}(x, r)$, which reflects the *primary selection* given by the fitness functions f and K . On longer, evolutionary time scales, the population evolves through *secondary selection*, i.e., by adaptive mutations modifying its mating range w_μ [32]. We study this process starting from a spatially uniform initial state with random mating. A single step involves an initially small mutant population that invades the resident population and eventually becomes a new stationary state $\bar{N}(x, r)$ with different trait and mating characteristics. At each step we evaluate whether a stationary state $\bar{N}(x, r)$ with given w_μ is unstable with respect to a small mutant population $n(x, r; t)$ with different mating range. Successful mutants are found to invade the resident population completely, producing a new stationary state. A possible dependence $w_\mu(x)$ due to a linkage disequilibrium, not taken into account here, is expected only to enhance the selection pressure towards assortativity. If adaptive substitutions are sufficiently rare, an evolutionary pathway can be represented as a sequence of intermediate stationary states leading to an evolutionary stable final state $\bar{N}_{\text{es}}(x, r)$ [33]. Along the pathway, the number of adaptive steps parametrizes evolutionary time. More generally, the mating range w_μ may be thought of as a further quantitative trait, the population state being described by a joint distribution $N(x, w_\mu, r)$. The distribution of w_μ is strongly peaked, which justifies the approximation of Eq. (2). The average value of w_μ evolves along fitness gradients towards the final state. Generic evolutionary stable states are found to have either random or strongly assortative mating.

Interesting variations in the internal structure of the model are related to the mating preference. It can depend on ecologically neutral but inheritable traits such as mating time, marker traits, and in all cases one may observe phenotypic differentiation [12, 13, 14, 34, 35]. In smaller populations some individuals may be unable to mate. Assortativity restricts the number of possible mates and should be disfavored under such circumstances. With some modification of Eq. (6) this effect can be studied and it turns out that certain types of reproductive isolation are actually favored [10, 34].

Unlike in our model inheritance in sexual population dynamics is often modelled genetically explicit. The classical approach is to consider a locus with two alleles, say a and A , and under which conditions preferentially homozygous subpopulations develop [5]. In computer simulations longer “genomes” can be used, typically two strings of L

bits with the “alleles” 0 and 1. Genome space is then very large, 2^{2L} , and a common way to follow the evolution of a population are simulation of so called individual based models (IBMs), [13, 14, 26]. For their evaluation population characteristics are sampled over large populations, long times, and many independent runs.

Based on phenotypes but closely related to genetics is the so called hypergeometric model [12, 28, 27, 30], where the phenotype of an individual with $2L$ loci is a quantitative trait proportional to the number of one type of alleles, e.g.

$$x = \sum_{\nu=1}^{2L} \sigma_{\nu} \in \{0, 1, \dots, 2L\}, \quad (8)$$

and the alleles are $\sigma_{\nu} \in \{0, 1\}$. If all genotypes mapping onto a phenotype are equally probable in a population, one can derive the probability $C(x|yz)$ for a couple with phenotypes y and z to have offspring with x : explicitly for a haploid and to a very good approximation for a diploid genome [28, 27]. Going one step further away from the underlying genetic concept leads to models of Quantitative Genetics [29] one of which is ours.

Generally such models neglect gene fixation. Also the hypergeometric model [12, 28, 27, 30] may be invalidated as the central assumption of equiprobability of the various genotypes contributing to one phenotype can fail [31]. But the same difficulty also arises for IBMs, as e.g. in [13, 14, 26], where only a “good” choice of mutation rate, population and genome size allows for meaningful dynamics with respect to the question of speciation. It is in these cases, that the phenotype related hypergeometric model and also quantitative phenotypic models as ours behave similarly and thus remain meaningful.

In Figure 2 we show some examples of $C(x|y, z)$ as functions of the offspring’s phenotype x for fixed phenotypes of mother and father, obtained by sampling over an IBM with genome length $2L = 64$, population size 16384, random mating, run for 10^7 generations. Phenotypes are given by Eq. (8). The children’s phenotypes are distributed around values $\bar{x}(y, z) = (y + z)/2$ with a (nearly Gaussian) distribution whose widths w_C are practically independent of the parents’ phenotypes. In panel (a) are examples for three values of $z = y$, in panel (b) for values $z = 2L - y$, such that the parents’ mean phenotypes are all identical $\bar{x} = L$. Panel (c) shows a long time average of the proportion of 1-alleles in the entire model genome compared to the values observed at the $2L$ model loci. These simulations show that the elementary combinatorial rules of inheritance on the genome level used in typical IBM simulations can quite well be approximated on the phenotype level by continuous functions for $C(x|y, z)$. The maximum value \bar{x} and the width w_C may be subject to corrective terms, but the principle structure of $C(x|y, z)$ remains valid.

In fact it turns out that the precise functional form of the interactions does not matter too much. We have also studied alternative forms of faster or weaker decay, e.g., $f(x, r) \sim \exp(-(x/w_f)^4)$, $\beta(x) \sim \exp(-(x/w_\beta)^2)$, $\mu(x) \sim \exp(-x/w_\mu)$. Important are the length scales in internal and external space: the inheritance uncertainty w_C , the competition range w_β , the resource width w_f , habitat heterogeneity x_0 , extent of habitatvariation r_0 , and migration range r_λ . Their combination and mutual relation decides about reproductive separation of the population into two or more subpopulations.

Results

We first discuss the special case where $f(x, r) \equiv f(x)$ and $N(x, r; t) \equiv N(x; t)$ do not depend on the spatial coordinate r , which requires $x_0 = 0$, and we consider a spatially

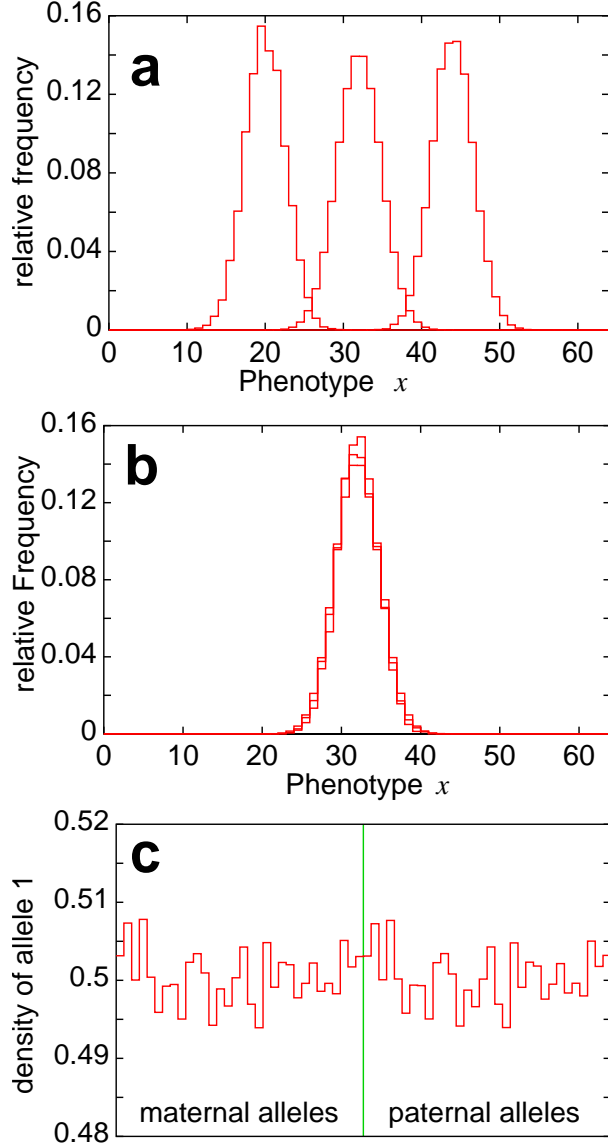


Figure 2: Examples of $C(x|y, z)$ sampled from a simulation of 16384 randomly mating individuals with genome length $2L = 64$ over 10^7 generations with mutation probability 10^{-3} per locus and generation. (a) Examples for $y = z = 20, 32$, and 44 . (b) Same z , but $y = 2L - z$. (c) Allele frequencies of 1's at the single loci differ by less than 1% from the average value $1/2$.

averaged “mean field” version of the model. Also in this limit sympatric speciation can become manifest, analogous to the results of the IBM in Refs. [13, 14] which is set in a similar ecological frame. For all evaluations we assumed the ecological interactions to extend over a wider range than the inheritance uncertainty, $w_C < w_f$ and $w_C < w_\beta$. During its adaptation the assortativity range w_μ varies, but it remains larger than w_C .

Evolving reproductive isolation can lead to separation into subpopulations. Equilibrium profiles of Eq. (2) are shown in Fig. 3, in panel (a) a unimodal population for random mating, in panel (b) a bimodal under mating assortativity after evolutionary adaptation of w_μ . For a large enough relative width of the habitat $w_f/w_\beta > 1.1$ the population evolves into a speciating state as in (b), otherwise it remains unseparated.

For given parameters w_C, w_β, w_f there may be a range of w_μ , where both a unimodal (as in Fig. 3(a)) and a bimodal population (as in Fig. 3(b)) are stable fixed points of

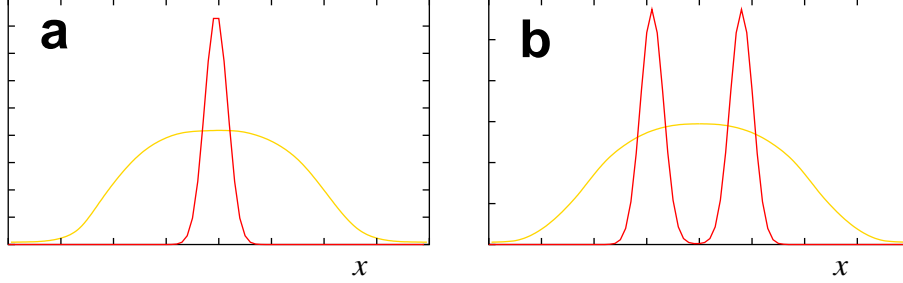


Figure 3: Fixed point configurations for Equation (2). (a) weak mating preference gives unimodal population structure, (b) strong mating preference allows for bimodal population structure. The phenotypic scale is indicated by the resource curve $f(x)$ plotted in light gray, the vertical scale of population density is arbitrary.

Eq. (2). As assortativity gets stronger (decreasing w_μ) the unimodal profile (Fig. 3(a)) becomes less stable. It is interesting to note that the transition between a unimodal and a bimodal population density is not a *gradual* process but a *fast switch* at a critical assortativity range w_μ . The switch occurs on the time scale of population dynamics, much faster than the evolutionary adaptation of w_μ . Under conditions where the evolutionary stable w_μ can increase again (e.g. slow variation of w_f) one finds hysteresis between the jumps from uni- to bimodal populations and back.

A population profile as in Fig. 3(b) *cannot* be a stable fixed point of the asexual version, i.e., the limit $w_\mu \rightarrow 0$, of Eq. (2): The gap between the two parts of the population would fill up resulting in a wider unimodal population profile covering most of the accessible phenotype range [10]. When w_μ remains finite two peaks in the population profile having widths close to but mutual distance greater than w_μ are stabilized by sexual reproduction because it accumulates offspring closer to their maxima. By this effect sexual reproduction *helps* speciation.

We now turn to the general case. The spatial model dynamics generates differentiation of the population, which can be measured in two ways: (i) The *mating differentiation index* δ is defined as the actual rate of crossmating between two subpopulations at a given point r , normalized by the same rate with random mating. For any population state $N(x, r)$, the mating differentiation index δ (at the point $r = 0$ and between the subpopulations $x < 0$ and $x > 0$) is defined by

$$1 - \delta = \frac{1}{Z} \int_{y < 0} dy \int_{z > 0} dz \frac{1}{2} [m(y, z, 0)N(y, 0) + m(z, y, 0)N(z, 0)], \quad (9)$$

where Z is the same integral evaluated with random mating, i.e., with $\mu(y, z) = 1$ for all y, z . (Analogous measures can be defined for different r and different trait subpopulations). Here we monitor the two subpopulations $x < 0$ and $x > 0$ at the boundary between the left and right regions ($r = 0$). (ii) The *spatial differentiation index* χ is defined in terms of the “trait overlap” between the populations at two different points in space. Phenotypes x that are intrinsically viable at one of these points are distinguished from those that are merely advected by diffusion. The spatial differentiation index χ (evaluated at the points $-r_0/2$ and $r_0/2$) is defined by

$$1 - \chi = \frac{1}{\tilde{Z}(r_0/2)} \frac{1}{\tilde{Z}(-r_0/2)} \int dx N_v(x, -r_0/2) N_v(x, r_0/2) \quad (10)$$

where $\tilde{Z}(r) = \int dx N_v(x, r)$. A phenotype x is counted as intrinsically viable at the point r if $w_C \beta(0) N(x, r)^2 - \lambda \partial^2 N(x, r) / \partial r^2 > 0$, i.e., if a small nonzero population in the interval

$[x - w_C(x)/2, x + w_C(x)/2]$ could exist even without diffusive advection. In this case, we set $N_v(x, r) = N(x, r)$, otherwise $N_v(x, r) = 0$. Here we take the points $r = -r_0/2$ in the left region and $r = r_0/2$ in the right region. Both indices vary between 0 (no differentiation) and 1 (complete separation).

Following the differentiation in phenotype and space over evolutionary times, three main mechanisms can be identified. They are distinguished by the structure of their evolutionary stable final populations $\bar{N}_{es}(x, r)$, measured, for example, by the resulting differentiation indices δ_{es} and χ_{es} .

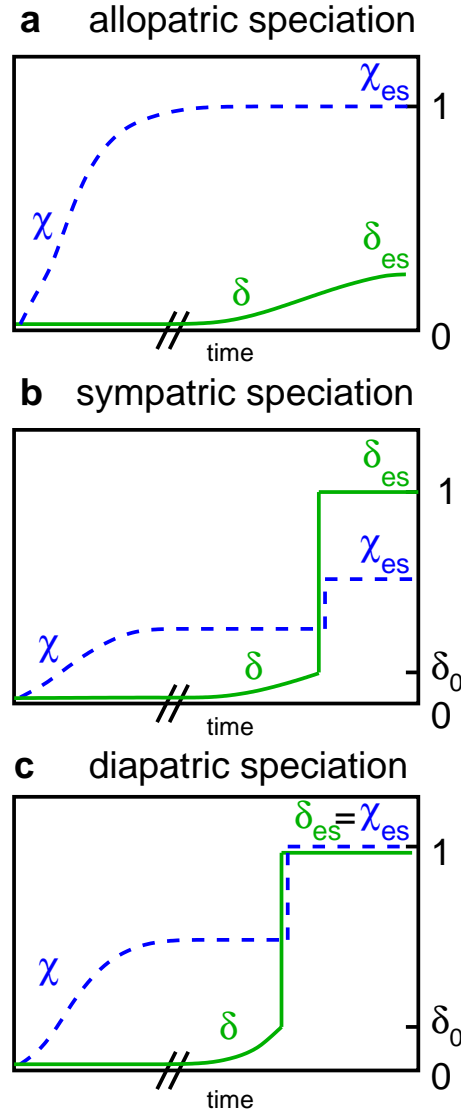


Figure 4: Three mechanisms of speciation can be distinguished by the time dependence of the mating differentiation index δ and the spatial differentiation index χ (see text). The initial population has random mating ($\delta = 0$) and is spatially homogeneous ($\chi = 0$). Primary selection with random mating (left part of the diagrams) is followed by secondary selection on the mating range w_m (right part of the diagrams). (a) **Allopatric speciation:** Continuous evolution by primary selection towards spatial segregation ($\chi_{es} = 1$) without reproductive isolation ($\delta_{es} < 1$). (b) **Sympatric speciation:** Discontinuous evolution towards reproductive isolation ($\delta_{es} = 1$) without spatial segregation ($\chi_{es} < 1$). (c) **Diapatric speciation:** Discontinuous, cooperative evolution towards reproductive isolation ($\delta_{es} = 1$) and spatial segregation ($\chi_{es} = 1$).

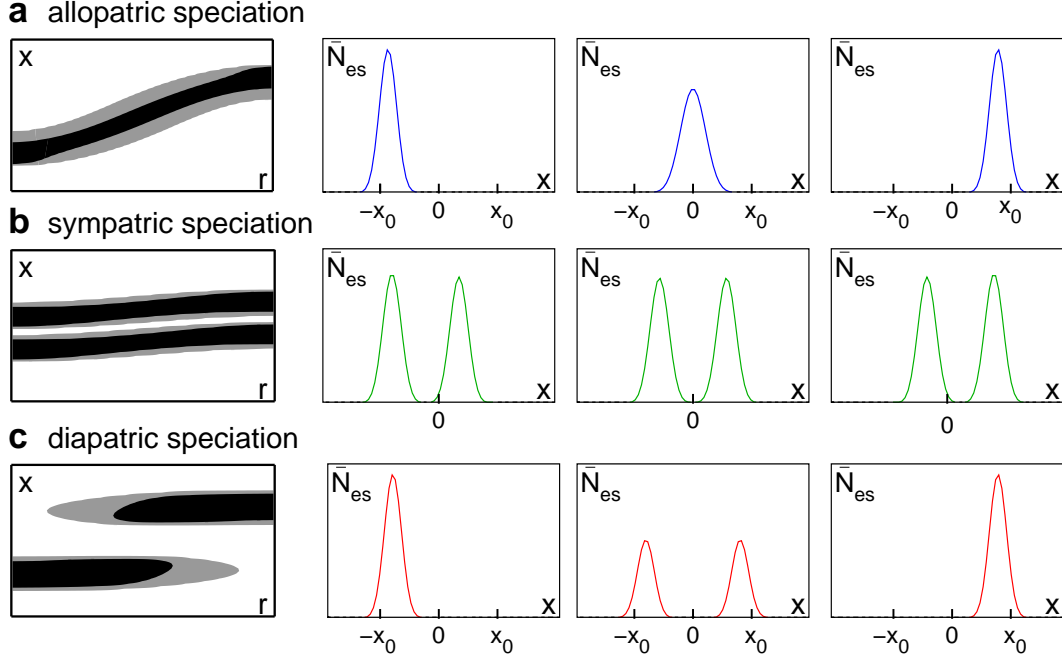


Figure 5: Evolutionary stable populations after speciation. Left column: Populated regions in the (x, r) plane, given by $\bar{N}_{\text{es}}(x, r) > 0$. Intrinsically viable phenotypes (shown in black) are distinguished from those advected by diffusion (grey). Right three columns: trait distributions $\bar{N}_{\text{es}}(x, r = -r_0/2)$ (left region), $\bar{N}_{\text{es}}(x, r = 0)$ (boundary between left and right region), and $\bar{N}_{\text{es}}(x, r = r_0/2)$ (right region). (a) **Allopatric speciation**: One contiguous population cluster, unimodal trait distributions, species boundary with hybrids. (b) **Sympatric speciation**: Two disjoint clusters, bimodal trait distributions. (c) **Diapatric speciation**: Two disjoint clusters, trait distributions unimodal within the regions and bimodal at the boundary, species boundary without hybrids.

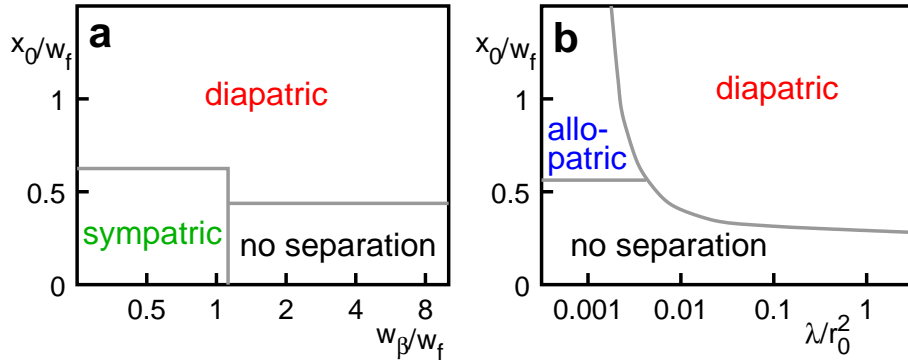


Figure 6: Phase diagram of speciation, specifying the mechanism as a function of the effective environment heterogeneity x_0/w_f , the effective competition range w_β/w_f , and the diffusion coupling between the regions, λ/r_0^2 . (a) Cross-section in the variables w_β/w_f and x_0/w_f at fixed $\lambda/r_0^2 = 0.01$. (b) Cross-section in the variables λ/r_0^2 and x_0/w_f at fixed $w_\beta/w_f = 2.0$. Diapatric speciation is the generic mechanism in heterogeneous environments with diffusive coupling.

Allopatric speciation shows a gradual increase of the spatial differentiation index χ up to $\chi_{\text{es}} = 1$, see Fig. 4(a). This expresses the patching of small- x phenotypes into the left region and large- x phenotypes into the right one. The spatial adaptation of traits

involves primary selection by the fitness function $f(x, r)$ only and occurs independently of mating behavior. Since there is no sufficient selection pressure towards assortativity, the mating differentiation δ_{es} remains small. The corresponding evolutionary stable population $\bar{N}_{\text{es}}(x, r)$ is a contiguous cluster in the (x, r) plane as shown in Fig. 5(a). At a given point r , the trait distribution is unimodal and centered around the local fitness maximum $x_f(r)$. There is a limited gene flow between the large- x and small- x subpopulations, which is maintained by the intermediate phenotypes near the boundary ($r = 0$).

Sympatric speciation is characterized by an increase of mating differentiation up to complete reproductive isolation; see Fig. 4(b). The index δ jumps discontinuously from a value $\delta_0 < 1$ to $\delta_{\text{es}} = 1$, implying that stationary population states with $\delta_0 < \delta < 1$ cannot exist. The speciation is driven by secondary selection involving the frequency-dependent fitness K , just as in previous models of strict sympatry. Spatial variations are irrelevant, and the spatial differentiation remains incomplete ($\chi_{\text{es}} < 1$). The evolutionary stable population $\bar{N}_{\text{es}}(x, r)$ shown in Fig. 5(b) consists of two disjoint clusters, corresponding to a bimodal trait distribution at every r . The gene flow between these subpopulations is suppressed by assortative mating. In particular, there are no hybrids near the boundary ($r = 0$).

Diapatric speciation is the co-evolution of assortative mating and spatial segregation by secondary selection. The indices δ and χ jump to $\delta_{\text{es}} = \chi_{\text{es}} = 1$ simultaneously, leading to an evolutionary stable state with reproductive isolation and patching into the left and right region, see Fig. 4(c). Prior to the jump, the spatial segregation is prevented by diffusive coupling between the regions. It becomes possible only once reproductive isolation is established. The population $\bar{N}_{\text{es}}(x, r)$ of Fig. 5(c) has two disjoint clusters. The trait distribution is unimodal within both regions and bimodal near the boundary; there are again no hybrids. The suppression of the gene flow between the clusters is now two-fold, by reproductive isolation and by spatial separation.

Does a population actually speciate, and if so, by which mechanism? This turns out to depend largely on only three parameters, the effective environmental heterogeneity x_0/w_f , the effective competition range w_β/w_f , and the diffusive coupling between the regions, λ/r_0^2 . (Here we have chosen w_f and r_0 as the basic scales in trait space and real space.) The “phase diagram” of Fig. 6 shows the mechanism of speciation as a function of these parameters. Allopatric speciation is possible only with a sufficiently large heterogeneity and a sufficiently small diffusive coupling (i.e., small λ or large region size r_0). Conversely, sympatric speciation requires a sufficiently small heterogeneity, as well as a sufficiently small competition range ($w_\beta/w_f < 1$). Diapatric speciation involves no restriction on the competition range, that is, it works for frequency-dependent as well as for density-dependent selection. It is seen to be the generic mechanism in many realistic environments with heterogeneities and diffusion.

This compares to the recent results of Ref. [26] where adaptive speciation is seen to generate a sharp geographical differentiation in an individual based model. Working over a wider range of parameters the present model is able to relate this diapatric mechanism to other modes of speciation by identifying their respective regions in terms of the relevant parameters.

The present model thus allows for a clear identification of the evolutionary mechanisms underlying speciation, of the dynamical patterns, and of the resulting population structures. Examples are the separation indices δ and χ (Eqs. (9) and (10)) and the distinction of intrinsically viable populations from populations merely advected by diffusion. Of course, this kind of differential analysis is very difficult in individual-based models, which always suffer from small discrete population sizes. On the other hand, the effect

of demographic stochasticity and other fluctuations can also be studied within the framework of Eq. (9) by adding a stochastic noise term. The evolutionary stable population densities $\bar{N}_{\text{es}}(x, r)$ are found to be stable under such perturbations. Stability or instability of stationary states $\bar{N}(x, r)$ become immediately apparent in differential equations such as (9) by their rates of convergence or divergence. The fast transition between coherent and segregated population states thus explains itself naturally from a simple analysis.

Discussion

In summary, our model suggests that speciation is a highly cooperative process involving the adaptive differentiation of a population in its ecological characters, its mating behavior, and its spatial structure. Diapatric speciation is the generic mechanism of fully coupled differentiation. It reduces to allopatric or sympatric speciation in special cases. All three mechanisms are part of a unified dynamical picture, conceptually different from the old dichotomy between sympatry and allopatry.

In classical observations, the spatial separation of newly formed species has often been regarded as the primary driving force of the speciation process. Our results call for a fresh look at the data and may offer a different interpretation in some cases. The diapatric mechanism involves spatial separation as an induced process, triggered by the reproductive isolation of subpopulations. This two-fold separation in phenotype and space between the emerging species cuts the gene flow more efficiently than the other mechanisms, which involve only one kind of separation.

Diapatric species boundaries are established and maintained by natural selection so no external barriers have to be postulated. They follow regional boundaries and are distinguished from the allopatric case by the efficient suppression of hybrids in the boundary zone during the primary speciation process. (Secondary reproductive isolation can suppress hybrids also in allopatry.) It is crucial to note that reproductively decoupled populations can adapt to spatial heterogeneities of smaller size than interbreeding ones. Diapatric speciation is also remarkably fast, since the loss of interbreeding takes place through an abrupt change of the stationary population state as discussed above. This transition is driven by natural selection, unlike the secondary mating differentiation mechanisms in allopatry, which are expected to operate by genetic drift and hence to be slower. Of course, the genetic fixation of permanent incompatibilities between the emerging species (postzygotic isolation) is always slow. Before that point, both reproductive and the spatial separation are reversible if the environmental conditions change, as has been confirmed by recent observations [36]. Hence, diapatric splits appear to be an efficient adaptation mechanism for sexual populations on small scales of space and time. Most of these splits are wiped out again on longer time scales, while a few develop into permanent speciation.

Acknowledgments

We are grateful to N. Barton, A. Hastings, M. Kirkpatrick, A. Kondrashov, and M. Rosenzweig for useful discussions and valuable comments. Particular thanks are due to D. Tautz for numerous comments throughout this work.

Correspondence and requests for materials can be addressed to both authors (emails: lassig@thp.uni-koeln.de, martin.rost@uni-bonn.de).

References

- [1] Meyer, A., Kocher, T.D., Basasibwaki, P., and Wilson, A.C. (1990) *Nature* **347**, 550-553.
- [2] Schliewen, U.K., Tautz, D., Pääbo, S. (1994) *Nature* **368**, 629-632.
- [3] Schliewen, U.K., Raßmann, K., Markmann, M., Markert, J., Kocher, T., and Tautz, D. (2001) *Molecular Ecology* **10**, 1471-1488.
- [4] Riço, C., and Turner, G.F. (2002) *Mol. Ecol.* **11** 1585-90.
- [5] Maynard Smith, J. (1966) *Am. Nat.* **100**, 637-650.
- [6] Antonovics, J. (1971) *American Scientist* **59** 593-599.
- [7] Dickinson, H., and Antonovics, J. (1973) *American Naturalist* **107** 256-274.
- [8] Rosenzweig, M. (1978) *Biol. J. Linn. Soc. (London)* **10**, 275-289.
- [9] Turner, G.F., and Burrows, M.T. (1995) *Proc. Roy. Soc. London B* **260**, 287-292.
- [10] Noest, A.J. (1997) *Proc. Royal Soc. London B* **264**, 1389-1393.
- [11] Geritz, S.E.H., Kisdi, É., Meszéna, G., and Metz, J.A.J. (1998) *Evolutionary Ecology* **12**, 35-57.
- [12] Kondrashov, A.S., and Kondrashov, F.A. (1999) *Nature* **400**, 351-354.
- [13] Dieckmann, U., and Doebeli, M. (1999) *Nature* **400**, 354-357.
- [14] Doebeli, M., and Dieckmann, U. (2000) *Am. Nat.* **156**, S77-S101.
- [15] Slatkin, M. (1980) *Ecology* **61**, 163-177.
- [16] The Greek prefix *δια-* often describes the process of a separation, e.g., *διατρέχειν*: to run apart.
- [17] Mayr, E. (1963) *Animal species and evolution*, Harvard University Press, Cambridge, MA.
- [18] Gavrillets, S., Li, H., and Vose, M.D. (2000) *Evolution* **54**, 1126-1134.
- [19] Bush, G.L. (1975) *Annual Review of Ecology and Systematics* **6** 339-364.
- [20] Endler, J.A. (1977) *Geographic Variation, Speciation and Clines*, Princeton University Press, Princeton, NJ.
- [21] Dieckmann, U., Metz, J.A.J., Doebeli, M., & Tautz, D. (Eds.) (2002) *Adaptive Speciation* Oxford University Press, Oxford, UK, Introduction and Epilogue.
- [22] Hutchinson, G.E. (1959) *Am. Nat.* **93**, 254-59.
- [23] Hendry, A.P., Wenburg, J.K., Bentzen, P., Volk, E.C., and Quinn, T.P. (2000) *Science* **290**, 516-518.

- [24] Rüber, L., Verheyen, E., and Meyer, A. (1999) *Proc. Natl. Acad. Sci. USA* **96**, 10230-10235.
- [25] Bush, G.L., Feder, J.L., Berlocher, S.H., McPheron, B.A., Smith, D.C., and Chilcote, C.A. (1989) *Nature* **339**, 346-349.
- [26] Doebeli, M., and Dieckmann, U. (2003) *Nature* **421**, 259-264.
- [27] Kondrashov, A.S. (1986) *Theor. Pop. Biol.* **29**, 1-15.
- [28] Doebeli, M. (1996) *J. Evol. Biol.* **9**, 893-909.
- [29] Bulmer, M.G. (1980) *The Mathematical Theory Of Quantitative Genetics*, Clarendon Press, Oxford, UK.
- [30] Shpak, M., and Kondrashov, A.S. (1999) *Evolution* **53**, 600-604.
- [31] Barton, N.H., and Shpak, M. (2000) *Theor. Pop. Biol.* **57**, 249-263.
- [32] Karlin, S., and McGregor, J. (1974) *Theor. Pop. Biol.* **5**, 95-103.
- [33] Hammerstein, P. (1996) *J. Math. Biol.* **34**, 511-532.
- [34] Kriener, B. (2003) Diplomarbeit, University of Cologne, Institute for Theoretical Physics.
- [35] Landé, R., (1981) *Proc. Nat. Acad. Sci. USA* **78**, 3721-3725.
- [36] Seehausen, O., van Alphen, J.J.M., and Witte, F. (1997) *Science* **277**, 1808-1811.